Nano Select

WILEY-VCH

nano select

RESEARCH ARTICLE OPEN ACCESS

CytroCell@PIL: A New Citrus Nanocellulose-Polymeric Ionic Liquid Composite for Enhanced Anion Exchange Membranes

Enrica Fontananova[1] | Rosaria Ciriminna[2] | Daria Talarico[1] | Francesco Galiano[1] | Alberto Figoli[1] | Gianluca Di Profio[1] | Raffaella Mancuso[3] | Bartolo Gabriele[3] | Christian S. Pomelli[4] | Lorenzo Guazzelli[4] | Giuseppe Angellotti[2] | Giovanna Li Petri[2] | Francesco Meneguzzo[5] | Mario Pagliaro[2]

[1]Istituto per la Tecnologia delle Membrane, CNR, Rende, Cosenza, Italy | [2]Istituto per lo Studio dei Materiali Nanostrutturati, CNR, Palermo, Peninsula, Italy | [3]Dipartimento di Chimica e Tecnologie Chimiche, Università della Calabria, Rende, Cosenza, Italy | [4]Dipartimento di Farmacia, Università di Pisa, Pisa, Italy | [5]Istituto per la Bioeconomia, CNR, Sesto Fiorentino, Firenze, Italy

Correspondence: Enrica Fontananova (enrica.fontananova@cnr.it) | Rosaria Ciriminna (rosaria.ciriminna@cnr.it)

Received: 21 November 2024 | **Revised:** 8 February 2025 | **Accepted:** 23 February 2025

Funding: This work was funded by the Ministero delle Imprese e del Made in Italy under the Piano Operativo della Ricerca “Ricerca e sviluppo sull’idrogeno” financially supported by the European Union—NextGenerationEU—M2C2 Investment 3.5, in the framework of the project PNRR Ricerca e Sviluppo sull’Idrogeno 2022–2025—Accordo di Programma “Idrogeno” (PRR.AP015.017.002), “Obiettivo 1—Produzione di idrogeno verde e pulito,” “LA 1.1.6—Sviluppo di materiali e componenti non contenenti materiali critici per elettrolizzatori anionici (AEM) operanti anche ad elevata pressione differenziale”. Work of Giovanna Li Petri was supported by MICS (Made in Italy—Circular and Sustainable) Extended Partnership and received funding from the European Union Next-GenerationEU (PNRR—Mission 4 Component 2, Investment 1.3—D.D.1551.11-10-2022, PE00000004). Work of Giuseppe Angellotti was supported by the SAMOTHRACE (Sicilian Micro and Nano TechnologyResearch and Innovation Center) Innovation Ecosystem using funding from European Union NextGeneration EU (PNRR—Mission 4 Component 2, Investment 1.5 (ECS00000022).

Keywords: alkaline water electrolysis | anion exchange membrane | CytroCell | green hydrogen | nanocellulose

ABSTRACT

Enhancement of alkaline water electrolysis requires the development of anion exchange membranes (AEMs) combining high permselectivity with a low resistance to ion transport and stability during prolonged contact with a concentrated alkaline solution. We now report that CytroCell@PIL, a mixed matrix membrane obtained by a synergic combination of CytroCell micronized citrus cellulose mixed at a 1 wt% load with a polymerizable ionic liquid (triethyl(4-vinylbenzyl)phosphonium tetrafluoroborate), shows vastly enhanced chemical and physical stability along with promising ionic conductivity. These findings establish the proof of concept toward the development of technical and economically viable large-area AEMs using polymeric membranes chemically and physically stabilized by CytroCell sustainably sourced via cavitation of industrial citrus processing waste conducted in water only.

1 | Introduction

Hydrogen is today recognized as a strategic energy vector for applications ranging from small- to large-scale power supply [1]. Alkaline water electrolysis (AWE) is already used to produce approximately 1%–2% of the 55 million tons of H_2 globally produced every year. Alkaline water electrolysis market is rapidly expanding, driven by the need to produce “green” hydrogen using electricity sourced from renewable energy sources (sun and wind in particular) [1]. Remarkably, indeed, as of late 2023, the installed capacity of electrolytic hydrogen stood at 860,000 tons for 1.1 GW installed power [2].

https://doi.org/10.1002/nano.70001

The main advantage of AWE with respect to the polymer electrolyte water electrolysis (PEMWE) is the possibility to use platinum-free catalysts [3–5]. The key difference between conventional AWE and AEM-based electrolysis is that the latter uses a non-porous polymeric membrane possessing intrinsic anionic conductivity, whereas in conventional AWE the porous electrode separator has no ionic conductivity, with conductivity being provided by KOH filling the pores of a separator. This allows to operate the cells at higher current densities with AEM-based AWE due to lower ohmic resistance, as well as to pressurize hydrogen electrochemically, easing storage and final utilization (reducing chemical risk) thanks to the non-porous nature of the polymeric membrane [4, 5].

The main bottlenecks to the development of AEM alkaline water electrolysis have been the materials used for making the membrane, and the lack of durability studies showing that AEM AWE technology can have comparable durability to conventional alkaline water electrolyzers [6]. In other words, the stability and durability of AEMs need to be significantly improved and current AEMs often require dilute KOH to prevent rapid degradation, indicating a limitation in their long-term usability in alkaline water electrolysis.

Polymeric ionic liquids (PILs) combine the unique conductivity properties of ionic liquids with the advantages of macromolecular crosslinked polymers stable in an aqueous environment. On the other hand, conventional ionic liquids are readily leached in water, which makes them unsuitable for application in water electrolysis. Merging good permselectivity with a low resistance to ion transport, PILs such as phosphonium ionic liquid–polyacrylate copolymers were recently shown to be suitable materials to make membranes for improved CO_2 separation [7].

The stability of polymeric materials in concentrated alkaline solution, however, in general is too low for long-term applications in AWE electrolyzers. State-of-the-art anion exchange membranes show poor chemical stability in alkaline solution, with degradation driven by the high nucleophilicity and basicity of OH^- ions [8].

Nanocellulose is well-known for its unique ability to impart great mechanical robustness to widely different polymers when added in small amounts [9]. The resulting composites, furthermore, are generally chemically stable due to the large number of hydroxyl groups at the surface of the cellulose nanofibrils readily forming molecular composites with many polymers. Nanocellulose-based membranes, for example, are promising for water purification based on pressure-driven filtration techniques, such as nanofiltration, ultrafiltration, and reverse osmosis [10]. In the field of AWE, (bacterial) nanocellulose has been used to produce flexible cathodes for hydrogen evolution via subsequent electrodeposition of Ni and Mo [11].

More recently, the first use of cellulose nanocrystals incorporated at 5 wt% loads along with 80 wt% zirconia into the hydrophobic polymer network of 15 wt% polysulfone resulted in a composite porous separator showing excellent stable performance in AWE for 300 h in 10% KOH electrolyte [12].

CytroCell is a new micronized cellulose reproducibly produced at low cost and in large amount (directly on a semi-industrial scale) from lemon (or any other *Citrus* fruit) industrial processing waste via hydrodynamic cavitation in water only [13]. The biomaterial consists of submicron long cellulose (partly esterified with citric acid) microfibrils whose section varies between about 110 and 420 nm, that dispersed in water show a large negative zeta-potential (−25 mV) [14]. Added in 1 wt% amount, for example, to pectin, CytroCell micronized cellulose enhances the structural and thermal properties of the resulting composite CytroCell@IntegroPectin cross-linked films [15]. Aiming to obtain a similar enhancement of the polymer properties, we chose to investigate the use of CytroCell as a functional additive of the aforementioned PIL membrane. The outcome is a new generation of AEMs that is promising toward the efficient implementation of AEM-based AWE.

2 | Methods and Materials

2.1 | Membrane Preparation and Characterization

The PIL used in this work was synthesized as previously reported [7]. The membranes were readily prepared via a green chemistry route based on photopolymerization of acrylic monomers in the presence of a small amount of CytroCell followed by casting. In detail, the monomeric styrene precursor functionalized with a triethylphosphonium group with the BF_4^- as a counter ion (triethyl(4-vinylbenzyl)phosphonium tetrafluoroborate, PIL4 (Figure 1a), with and without added CytroCell underwent photopolymerization by brief irradiation (3 min) with UV light using a low-pressure Hg lamp (Helios Italquarz, Cambiago, Italy). CytroCell (Figure 1b) was obtained as previously described directly on a semi-industrial scale processing about 30 kg of lemon processing waste kindly donated by a company (OPAC Campisi, Siracusa, Italy) in 180 L water [16]. Samples used were stored under N_2 in a refrigerator at 4°C for more than 3 years without any degradation. CytroCell was previously dispersed in water or in dihydrolevoglucosenone (CAS 53716-82-8; in the following reported with its Cyrene commercial name) according to the optimized procedure described in Section 2.2 (24 h stirring at room temperature followed by 30 min sonication).

The composition of the solutions employed before casting and photopolymerization are displayed in Table 1. Two composite membranes were prepared: one with water as the dispersing medium of CytroCell (MPIL4_CY_1) and another with Cyrene as solvent (MPIL4_CY_2). MPIL4 indicates the polymeric membrane prepared without CytroCell.

The five-step optimized and highly reproducible CytroCell@PIL membrane preparation route is outlined in Figure S1.

In detail, the procedure comprises five consecutive steps:

- CytroCell powder, previously ground in a mortar, is dispersed in the selected solvent (water or Cyrene) by stirring at room temperature for 24 h followed by 30 min sonication.
- The resulting CytroCell dispersion is added to a solution containing: 2-hydroxylmethacrylate (HEMA), dodecyltrimethy-

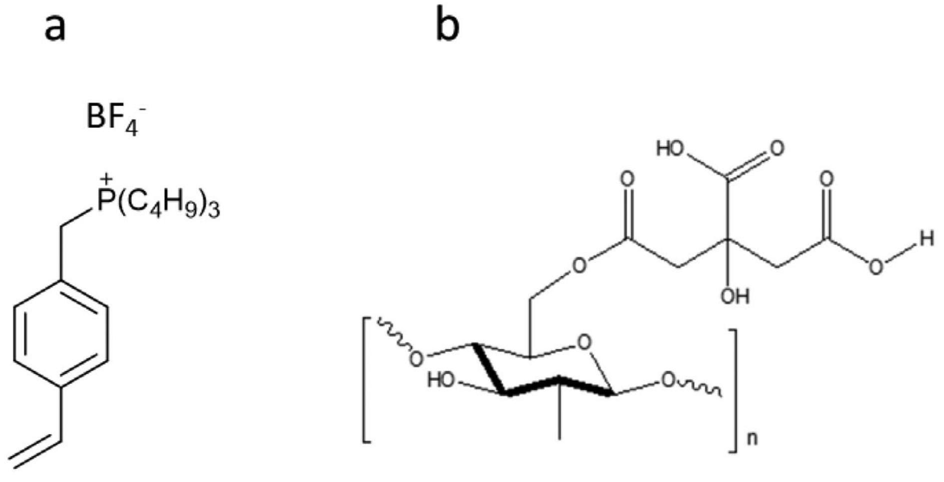

FIGURE 1 | Chemical structure of monomeric PIL4 (a), and CytroCell (b).

lammonium bromide (DTAB), and the polymerizable ionic liquid MPIL4. The resulting mixture is added with ethylene glycol dimethacrylate (EGDMA) and 2,2-dimethoxy-2-phenylacetophenone (DMPA) used as a photoinitiator.

- The solution is cast at a controlled thickness on a glass plate and then covered with a second glass plate spaced from the first one using a spacer. The reaction solution is photopolymerized via 3 min irradiation with UV-Vis light using the aforementioned lamp.
- The polymerized film is removed from the glass plate by immersion in water.
- The membrane thereby obtained was stored in water until use.

All the membranes were prepared in duplicate.

2.2 | Membrane Characterization

The resulting membranes were characterized by scanning electron microscopy (SEM) using an EVO MA10 microscope (Carl Zeiss, Oberkochen, Germany). In detail, in the SEM experiments, the membrane samples were coated with a thin gold layer before the analysis using a Sputtering Quorum Q 150R S device. Sections were fractured in liquid nitrogen.

TABLE 1 | Composition (wt%) of the casting solutions used to prepare the polymeric (MPIL4) and composite membranes (MPIL4_CY_1 and MPIL4_CY_2.[a]

Components	MPIL4	MPIL4_CY_1	MPIL4_CY_2
HEMA	50	50	50
H_2O	8.1	8	0
Cyrene	0	0	8.0
PIL	26	26	26
DTBA	13	13	13
EGDMA	2.3	2.3	2.3
DMPA	0.6	0.6	0.6
CytroCell	0	0.1	0.1

[a] MPIL4_CY_1: composite membrane prepared with water as dispersing medium of CytroCell; MPIL4_CY_2: composite membrane with Cyrene as solvent; MPIL4: triethyl(4-vinylbenzyl)phosphonium tetrafluoroborate.

The membranes were also characterized via electrochemical impedance spectroscopy (EIS). EIS experiments were carried out with an Autolab PGSTAT302N potentiostat/galvanostat equipped with a frequency response analyzer module in the frequency range 100000–1 Hz with a 10 mV signal amplitude (Metrohm Autolab, Utrecht, the Netherlands).

A four-electrode configuration was used to measure the in-plane conductivity with a BT-112 BekkTech conductivity cell (Scribner, Southern Pines, NC, USA). The four-electrode cells were placed in the Faraday cage during the measurements. The latter were conducted in water at temperatures between 25 and 70°C. The EIS spectra were processed with the Metrohm Autolab Nova 1.9.16 software to assess the ionic resistance of the membrane and calculate the conductivity as previously described [17].

EIS tests were carried out on the PIL-based membranes and on a commercial anion exchange membrane, Fumasep FAS-50 (FuMA-Tech, Germany). The membranes were conditioned in distilled water for at least 24 h before the in-plane conductivity test. Moreover, the test was carried out on the membrane treated as follows: (i) immersion in KOH 5 wt% for 24 h; (ii) rinsing in distilled water until neutrality to remove excess KOH.

Fourier transform infrared (FT-IR) analysis with an attenuated total reflectance method (ATR), was performed on the membranes using a Perkin Elmer Spectrum One spectrophotometer. The test was carried out on the pristine membrane and after treatment in KOH 5 wt%, as described above.

The mechanical properties of the membranes were measured in stress–strain elongation experiments using the ZWICK/ROELL Z 2.5 instrument.

The scanning transmission electron microscopy (STEM) samples of lemon CytroCell were prepared by suspending a small amount of powder in distilled water, treating them in an ultrasonic

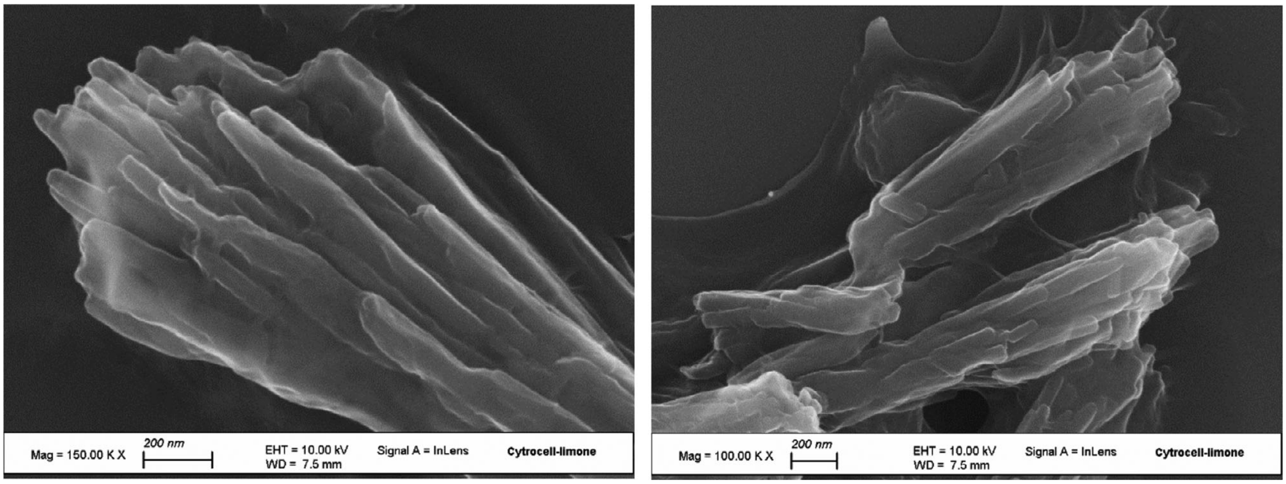

FIGURE 2 | FE-SEM images of lemon CytroCell.

bath, and drop casting them on carbon film-supported 200-mesh copper grids. All samples were dried at room temperature before analysis. The samples were then mounted on a grid and analyzed by using a Tescan MAGNA ultra-high resolution field emission scanning electron microscope (UHR FE-SEM) equipped with a STEM detector. The STEM analysis was performed in a bright field and at an accelerating voltage of 30 keV.

The samples for FE-SEM analysis were prepared by applying the water dispersions on silicon substrates and drying at room temperature. They were coated with a few nanometers of a conductive graphite layer. The FE-SEM images were recorded with a Zeiss high-spatial-resolution LEO Gemini 1530 field emission scanning electron microscope (FE-SEM). Images were all recorded in the secondary electron Inlens mode at an acceleration voltage of 10 keV.

The electron microscopy images taken on the same lemon CytroCell sample more than 2 years after the first TEM investigation [14] confirm that the lemon CytroCell fully retains its nanostructure after more than 2 years of storage at −20°C. The field emission scanning electron microscopy (FE-SEM) images in Figure 2 show the presence of microfibers with nanorod-like morphology. In agreement with the FE-SEM photographs, the STEM image in Figure 3 shows that the material is chiefly composed of elongated microfibers with a rod-like structure having a length of about 0.5–1.5 µm and a section of about 0.1–0.3 µm.

2.3 | Study of CytroCell Dispersion

As summarized in Table 2, CytroCell was dispersed in different solvents at 0.5% w/w load): water, dichloromethane (DCM), methanol (MeOH), ethanol (EtOH), isopropanol (*i*-PrOH), acetone, *N*,*N*-dimethylformamide (DMF), dimethylsulfoxide (DMSO), dimethylcarbonate (DMC) and cyrene (dihydroglucolevosenone). Aprotic polar solvent Cyrene [18] (Figure 4) is a green solvent suitable as alternative to conventional and highly toxic aprotic solvents *N*,*N*-dimethylacetamide, DMF, and *N*-methyl-2-pyrrolidinone (NMP).

Dispersions were obtained via one of three different procedures: stirring at room temperature (RT), stirring at 80°C, or via sonication using the compact ultrasound processor UP100H (100 W, 30 kHz) obtained by Hielscher (Teltow, Germany). Results in Table 2 show that DMSO was the most effective solvent for micronized CytroCell cellulose. However, its use raises concerns about its petrochemical origin, which may limit the sustainability of the membrane fabrication processes. Biobased Cyrene was selected due to its excellent sustainability profile, largely superior to that of DMSO, whose use should be reconsidered due to significant changes in cardiac and hepatic microtissues lately discovered [19]. Furthermore, Cyrene does not interfere with the photopolymerization reaction.

The dispersions of CytroCell in Cyrene remained stable for all 7 days of observation, whereas that in water required sonication (15 min) before use after 2 or 3 days. In each case, further reduction in size of the CytroCell particles grinding (using a pestle in a mortar) had a positive effect on improving CytroCell

FIGURE 3 | STEM image of lemon CytroCell.

TABLE 2 | Dispersion of CytroCell in different solvents at different temperatures and under sonication.

Solvent	Stirring at RT	Stirring at 80°C	Sonication
Water	Dispersed in 48 h	Dispersed in 24 h	Dispersed in 24 h
Cyrene	Dispersed in 48 h	Dispersed in 24 h	Dispersed in 24 h
DMC	Not dispersed	Limited dispersion	Limited dispersion
MeOH	Not dispersed	—	Limited dispersion
EtOH	Not dispersed	—	Limited dispersion
i-PrOH	Not dispersed	—	Limited dispersion
Acetone	Not dispersed	—	Limited dispersion
DMF	Limited dispersion	Dispersed in 24 h	Limited dispersion
DMSO	Dispersed in 24 h	Dispersed in 1 h	Dispersed in 1–2 h

dispersion. The optimized dispersion procedure with both water and Cyrene consists of merging mechanical stirring at room temperature for 24 h with 30 min sonication.

3 | Results and Discussion

The SEM photographs unveil a dense microstructure for all the membranes (Figure 5) showing evidence of the excellent solvent power of cellulose-derived Cyrene for the CytroCell cellulose nanorods. The SEM images of both the surface and the cross-section (Figure 6c,f) of the MPIL4_CY_2 membrane employing Cyrene as the only CytroCell solvent are homogeneous and devoid of aggregates.

On the other hand, the aggregates unveiled in the SEM images of MPIL4_CY_1 (Figure 6b,e) are likely due to undissolved CytroCell nanorods that in water are not sufficiently dispersed.

Compared to conventional cellulose nanocrystals extracted from cellulosic biomass using concentrated H_2SO_4 at high temperatures [20], lemon CytroCell, has a low crystallinity index of just 0.33 (due to the extreme pressure and temperature values of the imploding cavitation bubbles) and an open, mesoporous structure with 1.64 nm pore size and good water holding capacity (8 g_{water}/g_{cell}) [13].

Showing evidence of the remarkable stabilization effect of the CytroCell nanocellulose, Figure 6 displays a photograph of the unmodified MPIL4 membrane and of the corresponding membrane functionalized with CytroCell dispersed in water (MPIL4_CY_1) after immersion in a KOH 5 or 30 wt% aqueous solution for 24 h after washing with water till neutrality to remove the large base excess.

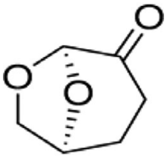

FIGURE 4 | Chemical structure of cyrene.

The unmodified MPIL4 membrane darkens especially in the more concentrated KOH solution because of the formation of a complex between the phosphonium groups and base, as confirmed by the FTIR spectra (Figures S2 and S3) showing an increase in the intensity of the phosphonium group (P-C stretching at 1237 cm^{-1}) with respect to the signal of the carbonyl group in hydroxylmethacrylate (C═O stretching at 1713 cm^{-1}). On the other hand, the membrane modified with 1 wt% CytroCell only retained its clear and transparent original appearance without any relevant change in the relative absorbance of the phosphonium group (Table 3).

We partly ascribe this exceptional stabilization effect to the antioxidant activity of the citric acid groups chemically bound to the C6 groups of the cellulose chain [13]. Such groups are formed via esterification reaction of the primary hydroxyl group of the cellulose fibrils with citric acid abundant in wet lemon processing waste under the extreme conditions created in the imploding cavitation bubbles eventually affording partly esterified nanocellulose fibrils. Citric acid indeed is a powerful antioxidant widely employed by the food and beverage industries to protect widely different foodstuffs and beverages from oxidative degradation preserving for example, the aspect (texture and color) and the organoleptic qualities of foodstuff, due to its ideally suited safety and health profile [21].

Along with the aforementioned high stability in concentrated KOH aqueous solution and improved mechanical stability, the other result that potentially opens the route to the use of CytroCell@PIL membranes as AEM in alkaline water electrolysis is shown in Figure 7.

The impedance measurements indeed show that the conductivity of the membranes increases with the temperature. The composite membranes prepared with water or Cyrene as dispersing medium of the CytroCell (MPIL4_CY_1 and MPIL4_CY_2, respectively) are less conductive than the polymeric MPIL4 membrane, due to the presence of acid groups in the bound citric acid groups that following contact with concentrated base deprotonate forming cation exchange centers in the CytroCell structure molecularly intertwined in the PIL polymeric structure. Said groups may interfere with the phosphonium anion exchange groups in PIL slightly lowering the conductivity.

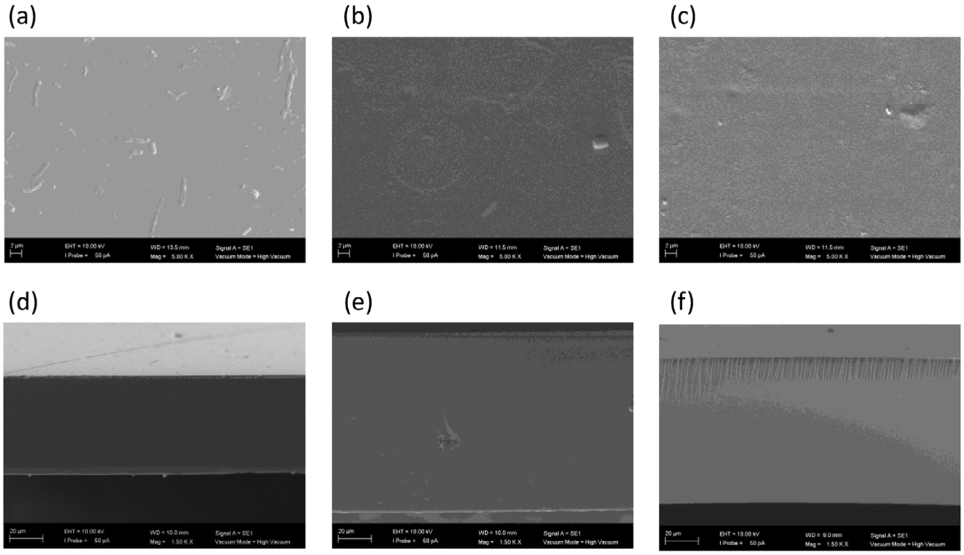

FIGURE 5 | Top: SEM photographs of the membrane surface: (a) unmodified polymeric membrane (MPIL4), (b) membrane modified with CytroCell dispersed in water (MPIL4_CY_1), (c) membrane modified with CytroCell dissolved in Cyrene (MPIL4_CY_2). Bottom: SEM photographs of membrane cross-section: (d) MPIL4, (e) MPIL4_CY_1, (f) MPIL4_CY_2.

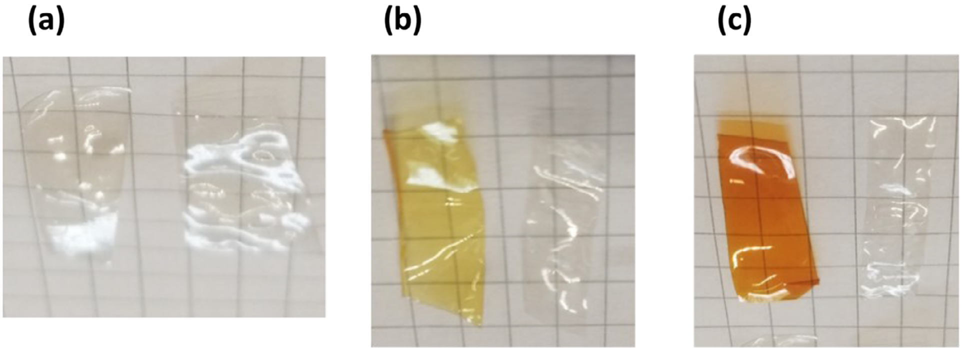

FIGURE 6 | Image of the polymeric membrane MPIL4 (on the left in each photo) and the membrane modified with CytroCell MPIL4_CY_1 (on the right in each photo): (a) as prepared, (b) after immersion in KOH 5 wt% and (c) KOH 30 wt% for 24 h.

However, the reinforcing effect of the CytroCell in a strong basic medium vastly exceeds the slight detrimental effect on conductivity. Whereas in the case of the unmodified MPIL4 membrane, the conductivity of the membrane following 24 h treatment with KOH 5 wt% significantly decreases (green curve in Figure 7), in the CytroCell@PIL membrane MPIL4_CY_1 functionalized with CytroCell the treatment with concentrated base leads to a significant *increase* in the conductivity (purple curve in Figure 8) at all investigated temperatures. Eventually, the composite membrane modified with CytroCell MPIL4_CY_1 becomes nearly as conductive as the MPIL4 membrane, not in contact with the concentrated base (grey curve in Figure 7).

Finally, a comparison of the mechanical properties of the unmodified polymeric membrane (MPIL4) and membrane modified with CytroCell (MPIL4_CY_1), clearly shows that the addition of CytroCell nanocellulose at modest 1 wt% load results in >60% higher elastic modulus (Table 4).

TABLE 3 | Ratio of the FTIR signals at 1237 and 1713 cm^{-1} in the unmodified polymeric membrane (MPIL4) and membrane modified with CytroCell dispersed in water (MPIL4_CY_1) before and after treatment with concentrated KOH (5 wt%) for 24 h.

Membrane	**Absorbance@1237 cm^{-1}/ Absorbance@1713 cm^{-1}**
MPIL4 (pristine)	0.61
MPIL4 (treated)	0.83
MPIL4_CY1 (pristine)	0.70
MPIL4_CY1 (treated)	0.70

Further highlighting the reinforcing action of the cellulose nanofibers on the PIL membrane, a nearly 10% reduction in the elongation at break was observed for the composite MPIL4_CY_1 membrane. The reinforcing effect of nanocellulose in composites with polymer is due to long nanofibers reaching the percolation threshold at low loading levels (between 1 and 6 vol.%, depending on the cellulose source) [22], when the rigid cellulose nanofibril

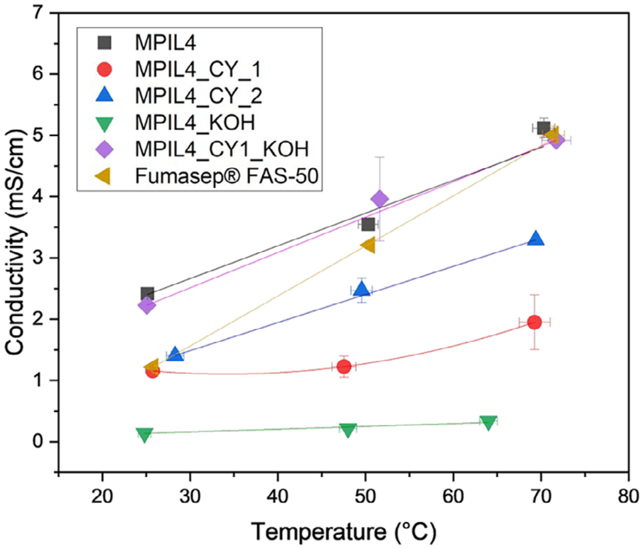

FIGURE 7 | Conductivity versus temperature plots for the unmodified polymeric membrane (MPIL4) and membranes modified with CytroCell (MPIL4_CY_1 and MPIL4_CY_2), and membrane MPIL4_CY_1 after treatment with KOH 5 wt% (MPIL4_CY_1_KOH).

TABLE 4 | Mechanical properties of the unmodified polymeric membrane (MPIL4) and membrane modified with 1 wt% CytroCell (MPIL4_CY_1).

Membrane	Elastic modulus (MPa)	Elongation at break (%)
MPIL 4	13 ± 2	46 ± 8
MPIL 4 CY_1	21 ± 3	42 ± 2

form a network within the nanocomposite due to percolation of the nanofibrils [9].

4 | Conclusions

In conclusion, we have discovered that citrus-derived micronized cellulose CytroCell sourced from waste lemon peel via hydrodynamic cavitation can be dispersed in water only and used as an additive at 1 wt% load to form composite membrane based on PIL such as phosphonium ionic liquid-polyacrylate copolymer. This composite membrane, dubbed herein CytroCell@PIL, shows exceptional stability in aqueous KOH, and good hydroxide conductivity. Furthermore, the addition of said small amount of CytroCell dispersed in water to the PIL precursor vastly improves also the mechanical stability of the resulting composite membrane. The latter result is important from a practical viewpoint because technologically mature AEMs employed in commercial electrolyzers will afford pressurized H_2 ready for storage and distribution as clean fuel [5].

Besides the development of new generation AEMs for alkaline water electrolysis, these findings are general and of relevance even to other key areas of contemporary research in renewable energy storage and utilization science and technology such as Li-based rechargeable batteries and fuel cells.

Finally, concerning practical feasibility, besides being waste-free and economically and environmentally sustainable, the production of CytroCell (and by-product IntegroPectin) from low-cost and abundant citrus processing waste via cavitation (hydrodynamic or acoustic) is intrinsically scalable [23]. Concerning membranes functionalized with CytroCell, we have not yet carried out an economic analysis of the membrane production method proposed. However, the solution casting technique is one of the most used at the industrial level for polymeric and mixed matrix membrane fabrication.

Acknowledgments

The authors thank Dr G. Di Carlo and Dr. C. Riccucci, Istituto per lo Studio dei Materiali Nanostrutturati, CNR, Montelibretti, for the FE-SEM and STEM measurements. This work was funded by the Ministero delle Imprese e del Made in Italy under the Piano Operativo della Ricerca “Ricerca e sviluppo sull’idrogeno” financially supported by the European Union—NextGenerationEU—M2C2 Investment 3.5, in the framework of the project PNRR Ricerca e Sviluppo sull’Idrogeno 2022–2025—Accordo di Programma “Idrogeno” (PRR.AP015.017.002), “Obiettivo 1—Produzione di idrogeno verde e pulito”, “LA 1.1.6—Sviluppo di materiali e componenti non contenenti materiali critici per elettrolizzatori anionici (AEM) operanti anche ad elevata pressione differenziale”. Work of Giovanna Li Petri was supported by MICS (Made in Italy—Circular and Sustainable) Extended Partnership and received funding from the European Union Next-GenerationEU (PNRR—Mission 4 Component 2, Investment 1.3—D.D.1551.11-10-2022, PE00000004). Work of Giuseppe Angellotti was supported by the SAMOTHRACE (Sicilian Micro and Nano TechnologyResearch and Innovation Center) Innovation Ecosystem using funding from European Union NextGeneration EU (PNRR—Mission 4 Component 2, Investment 1.5 (ECS00000022).

Conflicts of Interest

The authors declare no conflict of interest.

Data Availability Statement

The data that support the findings of this study are available from the corresponding author upon reasonable request.

References

1. J. C. Ehlers, A. A. Feidenhans’l, K. T. Therkildsen, and G. O. Larrazábal, “Affordable Green Hydrogen From Alkaline Water Electrolysis: Key Research Needs From an Industrial Perspective,” *ACS Energy Letters* 8 (2023): 1502–1509, https://doi.org/10.1021/acsenergylett.2c02897.

2. HydrogenCouncil, "Hydrogen Insights 2023," HydrogenCouncil accessed November 15, 2024, https://hydrogencouncil.com/wp-content/uploads/2023/12/Hydrogen-Insights-Dec-2023-Update.pdf.

3. N. Guillet and P. Millet, “Alkaline Water Electrolysis,” in *Hydrogen Production*, ed. Godula-Jopek, A. (Wiley-VCH, 2015), 117–166.

4. M. Kim, D. Lee, M. Qi, and J. Kim, “Techno-Economic Analysis of Anion Exchange Membrane Electrolysis Process for Green Hydrogen Production Under Uncertainty,” *Energy Conversion and Management* 302 (2024): 118134, https://doi.org/10.1016/j.enconman.2024.118134.

5. H. A. Miller, K. Bouzek, J. Hnat, et al., “Green Hydrogen From Anion Exchange Membrane Water Electrolysis: A Review of Recent Developments in Critical Materials and Operating Conditions,” *Sustainable Energy & Fuels* 4 (2020): 2114, https://doi.org/10.1039/c9se01240k.

6. C. Santoro, A. Lavacchi, P. Mustarelli, et al., “What Is Next in Anion-Exchange Membrane Water Electrolyzers? Bottlenecks, Benefits, and Future,” *ChemSusChem* 15 (2022): e202200027, https://doi.org/10.1002/cssc.202200027.

7. F. Galiano, R. Mancuso, L. Guazzelli, et al., "Phosphonium Ionic Liquid-Polyacrylate Copolymer Membranes for Improved CO_2 Separations," *Journal of Membrane Science* 635 (2021): 119479, https://doi.org/10.1016/j.memsci.2021.119479.

8. K. M. Meek and Y. A. Elabd, "Alkaline Chemical Stability of Polymerized Ionic Liquids With Various Cations," *Macromolecules* 48 (2015): 7071–7084, https://doi.org/10.1021/acs.macromol.5b01223.

9. K.-Y. Lee, Y. Aitomäki, L. A. Berglund, K. Oksman, and A. Bismarck, "On the Use of Nanocellulose as Reinforcement in Polymer Matrix Composites," *Composites Science and Technology* 105 (2014): 15–27, https://doi.org/10.1016/j.compscitech.2014.08.032.

10. P. R. Sharma, S. K. Sharma, T. Lindström, and B. S. Hsiao, "Nanocellulose-Enabled Membranes for Water Purification: Perspectives," *Advanced Sustainable Systems* 4 (2020): 1900114, https://doi.org/10.1002/adsu.201900114.

11. A. Abraham, V. R. Jothi, J. Lee, S.-C. Yi, and B.-I. Sang, "Bacterial Nanocellulose as a Green and Flexible Electrode Matrix for Efficient Hydrogen Evolution Reaction in Alkaline Conditions," *Cellulose* 27 (2020): 8135–8146, https://doi.org/10.1007/s10570-020-03327-y.

12. J. W. Lee, J. H. Lee, C. Lee, et al., "Cellulose Nanocrystals–Blended Zirconia/Polysulfone Composite Separator for Alkaline Electrolyzer at Low Electrolyte Contents," *Chemical Engineering Journal* 428 (2022): 131149, https://doi.org/10.1016/j.cej.2021.131149.

13. A. Scurria, L. Albanese, M. Pagliaro, et al., "CytroCell: Valued Cellulose From Citrus Processing Waste," *Molecules* 26 (2021): 596, https://doi.org/10.3390/molecules26030596.

14. S. Al Jitan, A. Scurria, L. Albanese, et al., "Micronized Cellulose From Citrus Processing Waste Using Water and Electricity Only," *International Journal of Biological Macromolecules* 204 (2022): 587–592, https://doi.org/10.1016/j.ijbiomac.2022.02.042.

15. A. Scurria, M. Pagliaro, G. Pantaleo, F. Meneguzzo, F. M. Giordano, and R. Ciriminna, "CytroCell Micronized Cellulose Enhances the Structural and Thermal Properties of IntegroPectin Cross-Linked Films," *ACS Applied Bio Materials* 5 (2022): 4942, https://doi.org/10.1021/acsabm.2c00658.

16. D. Nuzzo, L. Cristaldi, M. Sciortino, et al., "Exceptional Antioxidant, Non-Cytotoxic Activity of Integral Lemon Pectin From Hydrodynamic Cavitation," *ChemistrySelect* 5 (2020): 5066–5071, https://doi.org/10.1002/slct.202000375.

17. E. Fontananova, D. Messana, R. A. Tufa, et al., "Effect of Solution Concentration and Composition on the Electrochemical Properties of Ion Exchange Membranes for Energy Conversion," *Journal of Power Sources* 340 (2017): 282, https://doi.org/10.1016/j.jpowsour.2016.11.075.

18. D. Kong and A. V. Dolzhenko, "Cyrene: A Bio-Based Sustainable Solvent for Organic Synthesis," *Sustainable Chemistry and Pharmacy* 25 (2022): 100591, https://doi.org/10.1016/j.scp.2021.100591.

19. M. Verheijen, M. Lienhard, Y. Schrooders, et al., "DMSO Induces Drastic Changes in Human Cellular Processes and Epigenetic Landscape in Vitro," *Scientific Reports* 9 (2019): 4641, https://doi.org/10.1038/s41598-019-40660-0.

20. R. Prathapan, R. Thapa, G. Garnier, and R. Tabor, "Modulating the Zeta Potential of Cellulose Nanocrystals Using Salts and Surfactants," *Colloids and Surfaces A: Physicochemical and Engineering Aspects* 509 (2016): 11–18, https://doi.org/10.1016/j.colsurfa.2016.08.075.

21. S. K. Singh, R. Kaldate, and A. Bisht, "Citric Acid, Antioxidant Effects in Health," in *"Antioxidants Effects in Health*, ed. S. M. Nabavi, A. Sanches Silva (Elsevier, 2022), 309–322.

22. G. Siqueira, J. Bras, and A. Dufresne, "Cellulosic Bionanocomposites: A Review of Preparation, Properties and Applications," *Polymers* 2 (2010): 728–765, https://doi.org/10.3390/polym2040728.

23. R. Ciriminna, G. Angellotti, G. Li Petri, et al., "Cavitation as A Zero-Waste Circular Economy Process to Convert Citrus Processing Waste Into Biopolymers In High Demand," *Journal of Bioresources and Bioproducts* 9 (2024): 486–494, https://doi.org/10.1016/j.jobab.2024.09.002.

Supporting Information

Additional supporting information can be found online in the Supporting Information section.